British Journal of Pharmacology (1997) 120, 45–51

Somatostatin receptors in Neuro2A neuroblastoma cells: operational characteristics

[1,*,†]J.A. Koenig, *J.M. Edwardson & †P.P.A. Humphrey

†Glaxo Institute of Applied Pharmacology and *Department of Pharmacology, University of Cambridge, Tennis Court Road, Cambridge, CB2 1QJ

1 We have used somatostatin (SRIF) receptor subtype-selective ligands to determine some of the operational characteristics of somatostatin receptors in Neuro2A mouse neuroblastoma cells. The potent $SRIF_1$-receptor selective ligand, BIM-23027, was able to displace completely the specific binding of radioiodinated somatostatin, [^{125}I]-Tyr^{11}-SRIF-14, with a pIC_{50} of 10.3, suggesting that Neuro2A cells contain predominantly receptors of the $SRIF_1$ receptor group. The rank order of affinities for several somatostatin analogues tested in competition studies, together with the high affinity of BIM-23027, indicate that the majority of receptors in Neuro2A cells are of the sst_2 subtype.

2 The stable radioligand, [^{125}I]-BIM-23027, bound with high affinity ($K_d = 13$ pM, $B_{max} = 0.2$ pmol mg^{-1} protein) to Neuro2A cell membranes, but its binding was only partially reversible at room temperature and below. Thus at 4°C, only 36% of the bound ligand dissociated within 2 h. In contrast, 60% of the ligand dissociated at 15°C and 89% of the ligand dissociated at 37°C.

3 Equilibrium binding of [^{125}I]-BIM-23027 was partially (25%) inhibited by 10 μM GTP, and by 120 mM NaCl (42% inhibition) but this inhibition was increased to 75% when sodium chloride and GTP were added together. This effect of GTP and sodium chloride was also seen in dissociation experiments. After incubation to equilibrium with [^{125}I]-BIM-23027, dissociation was initiated with excess unlabelled ligand in the presence of GTP (10 μM) and sodium chloride (120 mM). Under these conditions 67% of the ligand dissociated at 4°C, 81% at 15°C and 93% at 37°C. Binding was totally inhibited by pretreatment of cells with pertussis toxin.

4 Functionally, BIM-23027 inhibited forskolin-stimulated cyclic AMP accumulation in a concentration-dependent manner with an IC_{50} of 1.0 nM and a maximal inhibition of 37%. This effect was abolished by pretreatment of the cells with pertussis toxin. However, unlike in studies reported with the recombinant sst_2 receptor, no rise in intracellular calcium concentration was observed with SRIF-14.

5 We conclude that Neuro2A cells provide a stable neuronal cell line for the study of functionally coupled endogenous somatostatin receptors of the sst_2 type. In addition, we have found that activation of the receptor is associated with ligand-receptor internalisation.

Keywords: Somatostatin receptors; Neuro2A cells; adenylyl cyclase inhibition; ligand binding; [^{125}I]-BIM-23027

Introduction

Somatostatin (SRIF) and its cell membrane receptors are widely distributed in the brain and periphery. Actions of somatostatin include modulation of hormone and transmitter release, cognitive and behavioural effects and the inhibition of cell proliferation (see Hoyer *et al*., 1994; 1995). Five somatostatin receptor genes have been cloned and the structures of the associated receptor proteins, termed $sst_1 - sst_5$, indicate that they all belong to the G-protein-coupled receptor super-family (Hoyer *et al*., 1995). These five receptors can be divided into two main groups on the basis of their affinity for small peptide ligands such as MK-678 (Raynor *et al*., 1993a,b). The $SRIF_1$ group consists of the sst_2, sst_3 and sst_5 receptors and shows high affinity for MK-678. The $SRIF_2$ group consists of the sst_1 and sst_4 receptors which show low affinity for MK-678 (Hoyer *et al*., 1994). SRIF-14 and SRIF-28 show similar potencies at all the receptor types. Somatostatin receptors couple to G_i/G_o G-proteins and can mediate inhibition of adenylyl cyclase (Patel *et al*., 1994), modulation of ion channel activity (Schweitzer *et al*., 1990; White *et al*., 1991; Kleuss *et al*., 1991; Meriney *et al*., 1994), increases in intracellular calcium levels (Akbar *et al*., 1994; Traina *et al*., 1996) as well as activation of phosphatases (Buscail *et al*., 1995).

Somatostatin receptors have been demonstrated in a number of pituitary cell lines, such as GH_4C_1 cells (Presky & Schonbrunn, 1988) and AtT20 cells (Hofland *et al*., 1995), and in gastrointestinal cells (Taylor *et al*., 1994; Prinz *et al*., 1994). We were interested in extending these studies by the examination of the characteristics of somatostatin receptors in a neuronal cell line. In recent years, a number of subtype-selective ligands for somatostatin receptors have become available (Raynor *et al*., 1993a,b). We have used some of these ligands to characterize the somatostatin receptors present in Neuro2A mouse neuroblastoma cells and here provide evidence that they are predominantly of the sst_2 type. However, a recent report of endothelin receptor binding (Wu-Wong *et al*., 1995) has suggested that binding of this high-affinity peptide is not readily reversible and work in our laboratories has suggested that this is also the case with somatostatin receptor agonist ligands (S. Holloway and W. Feniuk, unpublished observations). This would have particular implications for the design and interpretation of assays for receptor desensitization and ligand internalization (see Koenig *et al*., 1996). The characteristics of the binding of the recently-introduced radioligand, [^{125}I]-BIM23027, an sst_2 receptor-selective agonist, were therefore evaluated in order to enable appropriate design of functional assays. We have also investigated the coupling of somatostatin receptors to the transduction machinery in Neuro2A cells by measurement of the intracellular messengers, cyclic AMP and calcium.

Methods

Cell culture

Neuro2A cells were grown at 37°C in Dulbecco's modification of Eagle's Medium (DMEM), supplemented with 10%

[1] Author for correspondence

(by volume) foetal bovine serum and penicillin/streptomycin in 5% CO_2/95% humidified air. Cells were detached from culture flasks for passaging by a brief incubation with trypsin (0.5 mg ml^{-1}) and ethylenediaminetetraacetic acid (EDTA, 0.2 mg ml^{-1}) in phosphate-buffered saline (PBS composition, mM: NaCl 137, KCl 2.7, Na_2HPO_4 8.1, KH_2PO_4 1.5, $CaCl_2$ 0.9, $MgCl_2$ 0.5). Cells were passaged every 3–4 days.

Membrane preparation

Flasks containing confluent cells were washed twice with PBS and cells were detached from the flasks by incubation with PBS-EDTA. The cell suspension was centrifuged at 500 *g* for 5 min and the pellet was resuspended and homogenized in a Dounce homogenizer (25 strokes) in assay buffer (N-[2-hydroxyethyl]piperazine-N′-[2-ethanesulphonic acid] (HEPES) 10 mM, pH 7.4, $MgCl_2$ 11 mM, EDTA 1 mM) containing protease inhibitors (bacitracin 0.2 mg ml^{-1}, leupeptin 10 μg ml^{-1} and soybean trypsin inhibitor 1 μg ml^{-1}). The homogenate was centrifuged at 20,000 *g* for 20 min and the pellet was resuspended in assay buffer and frozen at −20°C.

Ligand binding assays

Membranes (5–15 μg) were incubated with [^{125}I]-BIM-23027 or [^{125}I]-Tyr^{11}-SRIF-14 in assay buffer (total volume 0.25 ml) for 2 h at 20°C unless otherwise indicated. For assays at pH 5.0, the assay buffer included HEPES 10 mM, pH 5.0, 2-[N-morpholino]ethane sulphonic acid (MES) 10 mM, $MgCl_2$ 11 mM and EDTA 1 mM. Non-specific binding was defined using 2 μM SRIF-14, and generally accounted for 25-35% of total binding at 0.05 nM [^{125}I]-BIM-23027 or [^{125}I]-Tyr^{11}-SRIF-14. The incubation was terminated by filtration through polyethyleneimine-soaked GF/C filters in a Brandel cell harvester. Filters were transferred to vials and counted in a gamma counter. For saturation analysis, seven different concentrations of [^{125}I]-BIM-23027 were used between 0.002 to 0.12 nM. Saturation experiments were analysed with the programmes EBDA and LIGAND (Munson & Rodbard, 1980). For association experiments, membranes were incubated with 0.05 nM [^{125}I]-BIM-23027 for various times at the appropriate temperature. For dissociation experiments, membranes were incubated with 0.05 nM [^{125}I]-BIM-23027 for 30 min at 37°C, and then dissociation was initiated by addition of an equal volume of buffer containing 4 μM SRIF-14. In some experiments the dissociation buffer also contained guanosine 5′ triphosphate (GTP, 10 μM) and sodium chloride (120 mM). Inhibition curves and association and dissociation kinetic experiments were analysed using GraphPad Prism. Inhibition data were fitted to the equation,

$$\text{Bound} = \frac{100}{1 + 10^{(\log[D] - \log(\text{IC}_{50}))}}$$

where [D] is the unlabelled ligand concentration.
pIC_{50} values quoted are equal to the $-\log IC_{50}$ value.
Association data were fitted to the equation,

$$Bound = \max imum(1 - e^{-k_{on,apparent}t})$$

$$\text{where } k_{on,apparent} = k_{+1}[D] + k_{-1}$$

Dissociation data were fitted to the equations,
one-site model: $Bound = proportion_1 e^{-k_{-1}t} + asymptote$
two-site model: $Bound = proportion_1 e^{-k_{-1}t} + proportion_2 e^{-k_{-2}t} + asymptote$

Where 'proportion' is the percentage of total binding which dissociated at rate '*k*' and 'asymptote' is the percentage of binding which could not be dissociated. The model which fitted the data best was determined by *F*-test.

Cyclic AMP measurements

Cells were grown to confluence in 225 cm^2 flasks. Cell monolayers were rinsed twice with PBS, detached from the flasks with PBS-EDTA (5 mM) and centrifuged at 500 *g* for 5 min. The cells were resuspended in DMEM and distributed into Eppendorf tubes. Each tube contained 0.27 ml of cell suspension (approximately 500,000 cells/tube). Cell density was determined by counting the cells with a Neubauer haemocytometer. Cells were incubated at 37°C for 15 min with 3-isobutyl-1-methylxanthine (IBMX, 0.5 mM). Forskolin (10 μM final concentration) was added with drugs where appropriate for 10 min at 37°C in a final volume of 0.3 ml. The incubation was terminated by addition of 10 μl HCl (10 M) followed by 10 μl NaOH (10 M) and 200 μl 1 M Tris-HCl, pH 7.4. The broken cells were pelleted by centrifugation at 12,000 *g* for 2 min in an Eppendorf centrifuge. The supernatant containing released cyclic AMP was removed and stored at −20°C.

Cyclic AMP was quantified through inhibition of the binding of 2 nM [^{3}H]-cyclic AMP to protein kinase A (Sigma, 5 μg/tube) and comparison with a standard calibration curve of known cyclic AMP concentrations from 0.5 to 16 pmol cyclic AMP in a total volume of 0.2 ml. The assay buffer contained Tris-HCl 50 mM, pH 7.4, EDTA 4 mM, NaCl 100 mM and 0.5% (w/v) BSA. The reaction mixture was incubated for 2 h at 4°C and the incubation terminated by filtration through polyethyleneimine-soaked GF/B filters in a Packard 96-tube Filtermate followed by 3 rinses with 1 ml ice-cold distilled water. The filters were dried and counted in 50 μl Microscint O using a Canberra-Packard TopCount scintillation counter. Protein content was determined according to Bradford (1976) with bovine serum albumin as the standard.

Intracellular calcium measurements

Cells grown on glass coverslips were incubated for 50 min with 3.3 μM Fura 2-acetoxymethyl ester in HEPES-buffered Krebs solution, pH 7.4, containing 1 mg ml^{-1} bovine serum albumin at room temperature. The coverslip was then mounted in a thermostated 1 ml cuvette in a Hitachi spectrophotometer. The cuvette was continuously perfused at 37°C with incubation buffer at 1.0–1.5 ml min^{-1}. Background autofluorescence was measured before loading cells with Fura-2.

Materials

[^{125}]-BIM-23027 (specific activity 2,000 Ci mmol^{-1}) and [^{125}I]-Tyr^{11}-SRIF-14 (specific activity 2,000 Ci mmol^{-1}) were obtained from Amersham International plc (Amersham, Bucks). Cell culture medium was from ICN Biomedicals (High Wycombe, Bucks), and foetal bovine serum was from GIBCO (Uxbridge, Middx). Pertussis toxin was from Calbiochem. Peptides were synthesised by Dr J. Kitchen's team, Chemistry Division, Glaxo Group Research: BIM-23027 (*cyclo*[N-Me-Ala-Tyr-D-Trp-Lys-Abu-Phe]), BIM-23056 (D-Phe-Phe-Tyr-D-Trp-Lys-Val-Phe-D-Nal-NH_2) MK-678 (*cyclo*(N-Me-Ala-Tyr-D-Trp-Lys-Val-Phe)) and L-362855 (*cyclo*[Aha-Phe-Trp-D-Trp-Lys-Thr-Phe). All other chemicals were from Sigma (Poole, Dorset). Sep-Pak Plus C18 minicolumns were obtained from Waters Chromatography (Watford Hertfordshire, U.K.).

Results

Ligand binding studies with [^{125}I]-Tyr^{11}-SRIF-14 and [^{125}I]-BIM-23027

In order to determine which somatostatin receptor types are present in Neuro2A cells, we examined the binding affinities of a number of agonists which show selectivity for the different receptors types. Initial experiments showed that BIM-23027 was able to displace all of the binding of [^{125}I]-Tyr^{11}-SRIF-14 to cell membrane homogenates with a pIC_{50} of 10.29 ± 0.03 (Figure 1a). The inhibition of [^{125}I]-BIM-23027 binding by a series of compounds was examined in competition studies (Figure 1b). The pIC_{50} values were (mean ± s.e.mean of three

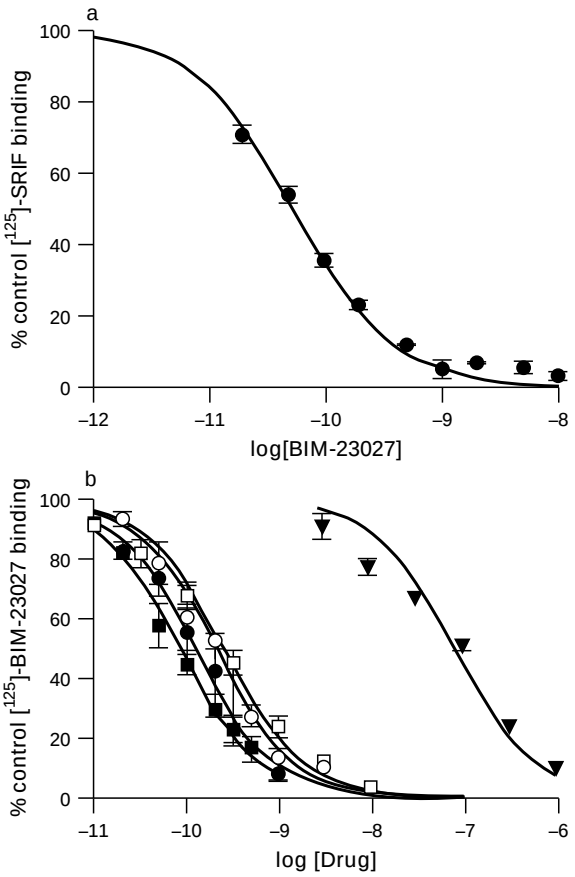

Figure 1 (a) Inhibition of specific [^{125}I]-Tyr^{11}-SRIF-14 binding by BIM-23027 in Neuro2A membranes. The pIC_{50} was 10.29 (IC_{50} = 51.5 pM). Values are means with s.e.mean of three separate experiments, each performed in triplicate. (b) Inhibition of specific [^{125}I]-BIM-23027 binding in Neuro2A membranes. The pIC_{50} values were SRIF-14, 9.9 (●); SRIF-28, 9.7 (○); MK-678, 10.1 (■); L-362855, 9.6 (□); BIM-23056, 7.1 (▼). In all cases the data were fitted best to a one-site displacement model with a Hill slope of unity.

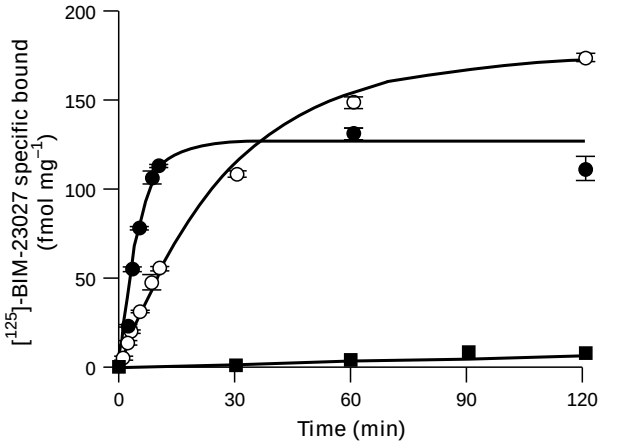

Figure 2 Association of [^{125}I]-BIM-23027 (0.05 nM) with membranes at either 4°C, 15°C or 37°C. Neuro2A membranes were incubated for various times with [^{125}I]-BIM-23027 (0.05 nM) at either 4°C (■), 15°C (○) or 37°C (●). Data are expressed as specific binding (fmol mg^{-1} protein) and represent a typical experiment, which was repeated three times with similar results. Means ± s.e.mean of triplicate determinations are shown. In these experiments, apparent association rates were 0.2 min^{-1} at 37°C and 0.04 min^{-1} at 15°C and the total binding was 174 fmol mg^{-1} protein at 15°C and 127 fmol mg^{-1} protein at 37°C.

Table 1 Association kinetic data for [^{125}I]-BIM23027 binding to Neuro2A membranes at either 15 or 37°C

Temp (°C)	$k_{(+1,\ apparent)}$ (min^{-1})	$k_{(+1)}$ (M^{-1} min^{-1})	*Maximum binding* (fmol mg^{-1} protein)
15	0.048 ± 0.005	*	127 ± 28
37	0.18 ± 0.018	3.46×10^9	100 ± 25

Values are the means (± s.e.mean) of 4 determinations.
*Not determined as not at equilibrium (see text).

determinations) SRIF-14, 9.91 ± 0.04; SRIF-28, 9.69 ± 0.02; MK-678, 10.08 ± 0.03; L-362855, 9.60 ± 0.04; BIM-23056, 7.09 ± 0.05. In all cases the data were fitted best to a one-site displacement model.

Further characterization of [^{125}I]-BIM-23027 binding

The kinetics of [^{125}I]-BIM-23027 binding were studied in membranes from Neuro2A cells at 4°C, 15°C and 37°C. The time course of binding is shown in Figure 2 and the derived association kinetic parameters are summarized in Table 1. Steady state was reached within 2 h at 15°C and within 30 min at 37°C. h.p.l.c. analysis of the free ligand after incubation in buffer at 15°C or 37°C showed that BIM-23027 was stable in buffer at 37°C for at least 4 h. Analysis of [^{125}I]-BIM-23027 using Sep-Pak cartridge chromatography (Koenig *et al*., 1996) after incubation with membranes for 2 h at 37°C also showed no generation of radiolabelled free amino acids.

Dissociation experiments revealed a considerable temperature-dependence (Table 2). At 37°C, bound radioligand dissociated almost completely (10.9 ± 5.7% ligand remained bound, n = 4) while in contrast at 15°C, 39.8 ± 2.9% (n = 5) of the ligand remained bound after 2 h and 63.9 ± 6.5% (n = 3) remained bound at 4°C (Figure 3). Inclusion of GTP (10 μM) or sodium chloride (120 mM) resulted in a reduction of equilibrium binding, which was increased by the addition of GTP and sodium chloride together (Figure 4). In order to determine the rate at which the radioligand dissociated in the presence of both GTP and sodium chloride, the membranes were incubated with [^{125}I]-BIM-23027 for 30 min at 37°C in their absence to allow binding to reach equilibrium, and then the amount of radioligand bound was measured at various times after addition of 10 μM GTP, 120 mM NaCl and 2 μM SRIF-14. When the dissociation was carried out at 4°C in the presence of GTP and sodium chloride, 67.2 ± 3.0% (n = 3) of the ligand dissociated while at 15°C in the presence of GTP and sodium chloride, 80.6 ± 0.9% (n = 5) of the ligand dissociated. When the temperature was increased to 37°C, 92.5 ± 3.9% (n = 4) of the ligand dissociated within 10 min (Figure 5). In the presence of GTP and sodium chloride dissociation could be best fitted to a two-phase exponential model. The dissociation rates are shown in Table 2.

Saturation analysis with [^{125}I]-BIM-23027 was performed at 37°C to determine the binding affinity and receptor density, avoiding possible artefacts due to the very slow dissociation at lower temperatures. The total number of binding sites was found to be 0.20 ± 0.05 pmol mg^{-1} protein with a K_D of 12.6 pM (pK_d ± s.e.mean = 10.90 ± 0.01 (n = 3) by saturation analysis, which agrees well with the K_D of 11 pM estimated from the association and dissociation rates (0.037 min^{-1}/ 3.46×10^9 M^1 min^{-1}). When the saturation analysis was performed at 15°C, the total number of binding sites was similar (0.29 ± 0.04 pmol mg^{-1} protein (n = 4)) but the apparent affinity was lower (K_D = 23 pM; pK_d ± s.e.mean = 10.6 ± 0.02).

Functional studies

BIM-23027 caused a concentration-dependent inhibition of forskolin-stimulated increase in cyclic AMP formation, with a

Table 2 Dissociation kinetic data for [^{125}I]-BIM23027 binding to Neuro2A membranes at various temperatures

Temp (°C)	k_{-1} (min^{-1})	*Proportion site 1* (%)	k_{-2} (min^{-1})	*Proportion site 2* (%)	*Asymptote** (%)	n
4	0.075±0.049	32.7±9.8			63.9±6.5	3
15	0.077±0.015	57.5±3.9			39.8±2.9	5
25	0.051±0.016	50.4±6.6			39.3±5.5	3
37	0.037±0.006	86.2±5.6			10.9±5.7	4
In the presence of GTP (10 μM) and sodium chloride (120 mM)						
4	0.40±0.12	65.9±7.8			32.8±3.0	3
15	4.1±0.6	54.3±2.1	0.095±0.014	26.3±1.7	19.4±0.9	5
25	undefined	55.8±4.4	0.032±0.009	39.6±3.6	4.6±3.4	3
37	2.8±1.2	49.3±7.6	0.083±0.029	43.1±6.2	7.5±3.9	4

Values are the means (±s.e.mean) of *n* determinations. *Asymptote refers to the remainder bound after 2 h.

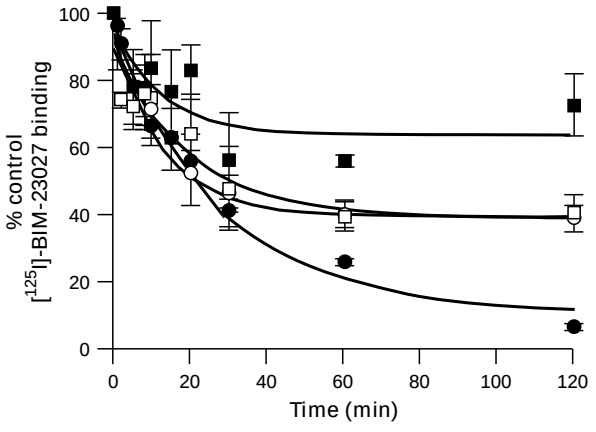

Figure 3 Dissociation kinetics of [^{125}I]-BIM-23027 binding to Neuro2A membranes at 4°C, 15°C, 25°C or 37°C. Neuro2A membranes were incubated with 0.05 nM [^{125}I]-BIM-23027 for 30 min at 37°C. Dissociation was initiated by addition of excess unlabelled SRIF-14, and allowed to proceed for various times at either 37°C (●), 25°C (□), 15°C (○) or 4°C (■). Data are expressed as a percentage of control (no dissociation buffer added and filtered immediately). The dissociation rates are given in Table 2. Values are means±s.e.mean of 3 (4°C, 25°C), 5 (15°C) or 4 (37°C) experiments.

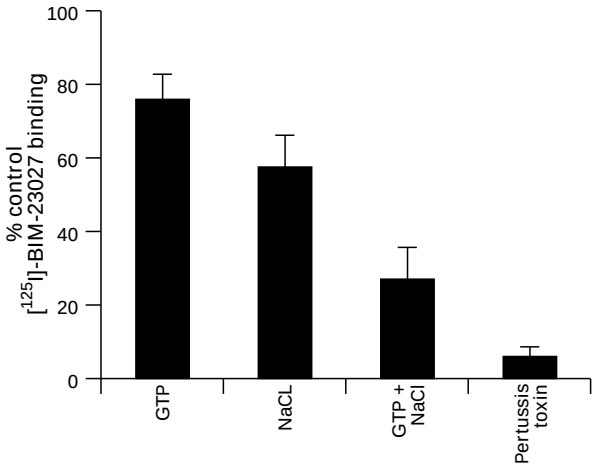

Figure 4 Effect of GTP (10 μM), NaCl (120 mM), GTP plus NaCl and pertussis toxin pretreatment (500 ng ml^{-1}, 16 h) on [^{125}I]-BIM-23027 binding to Neuro2A membranes at room temperature. Data are expressed as a mean percentage (with s.e.mean) of control; n=3 experiments except 2 experiments for pertussis toxin treatment where error bars represent the range.

maximum inhibition of 37±2% ($n=3$) and an IC_{50} of 1.0 nM ($pIC_{50}=9.0\pm0.2$, $n=3$; see Figure 6). This inhibition was abolished by pretreating cells overnight with 500 ng ml^{-1} pertussis toxin (Figure 6). SRIF-14 did not cause an increase in intracellular calcium, as measured by Fura-2 fluorescence, although the cells did respond to 10 μM adenosine 5′-triphosphate (ATP, Figure 7).

Discussion

We have investigated the operational characteristics of somatostatin receptors in Neuro2A mouse neuroblastoma cells using both binding and functional assays. Somatostatin receptors have been divided into two main types, $SRIF_1$ and $SRIF_2$ (Hoyer *et al*., 1995). We show here that the somatostatin receptor in Neuro2A cells has characteristics of the $SRIF_1$ type, as revealed by the extremely high affinity of MK-678. However, within the $SRIF_1$ group, there are three receptor subtypes, sst_2, sst_3 and sst_5. The order of potencies of a number of peptides suggests that the receptor in Neuro2A cells is of the sst_2 type. First, BIM-23027 has been shown to be a potent and selective sst_2 receptor agonist having 1000 times greater affinity at the mouse sst_2 receptor than the mouse sst_3 or rat sst_5 receptors (Raynor *et al*., 1993a,b). Indeed the radio-iodinated version of BIM-23027 has been recently introduced as a useful sst_2 receptor probe on account of its high degree of selectivity (Holloway *et al*., 1996; McKeen *et al*., 1996). The complete displacement of [^{125}I]-Tyr^{11}-SRIF-14 by very low concentrations of BIM-23027 and with a Hill slope of unity in this study is therefore entirely consistent with the receptor in Neuro2A cells being predominantly of the sst_2 type. However, given that BIM-23027 has some, albeit lower affinity for the sst_3 and sst_5 receptors we cannot exclude the possibility that there may be up to 10% of the binding sites contributed by sst_3 and sst_5 receptors (Raynor *et al*., 1993a,b). Raynor and colleagues also described several other peptides which can purportedly discriminate sst_2 receptors from the other receptor subtypes, sst_3 and sst_5, in the $SRIF_1$ group (Raynor *et al*., 1993a,b). These included BIM-23056 which has markedly higher affinity at sst_3 and sst_5 receptors than at sst_2 receptors and L-362,855 which is a potent sst_5 receptor agonist (Raynor *et al*., 1993b; O'Carroll *et al*., 1994; Patel & Srikant, 1994). Although there is some controversy about the precise relative potencies of such peptides they nevertheless provide useful drug tools if used circumspectly. The close similarity of the rank order of agonist potencies obtained in this study with that reported by McKeen and colleagues using the same radioligand with human recombinant sst_2 receptors adds further evidence for the presence of sst_2 receptors in Neuro2A cells and also demonstrates close similarities in the operational characteristics of mouse and human sst_2 receptors (Castro *et al*., 1996; McKeen *et al*., 1996). Indeed preliminary unpublished data from our laboratory using Western blotting techniques with an sst_{2a} receptor anti-

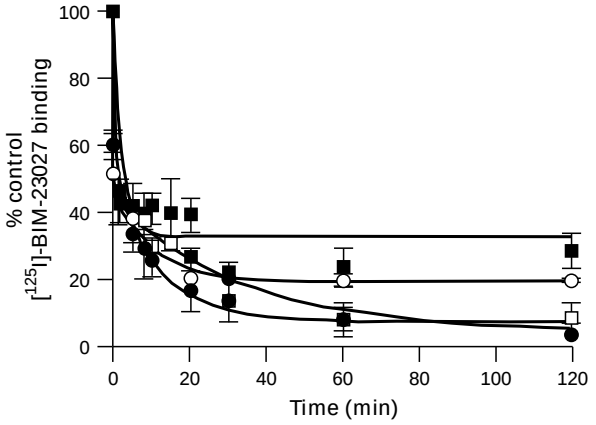

Figure 5 Dissociation of [^{125}I]-BIM-23027 from Neuro2A membranes in the presence of 10 μM GTP and 120 mM NaCl at either 4°C, 15°C, 25°C or 37°C. Dissociation was initiated by addition of excess unlabelled SRIF-14, 10 μM GTP and 120 mM NaCl and was allowed to proceed for various times at either 37°C (●), 25°C (□) 15°C (○) or 4°C (■). Data are expressed as a percentage of control (no dissociation buffer added and filtered immediately). In all cases except 4°C, the data were fitted best by a two-phase dissociation model. The dissociation rates are given in Table 2. Values are means from 3 (4°C, 25°C), 5 (15°C) or 4 (37°C) experiments ± s.e.mean.

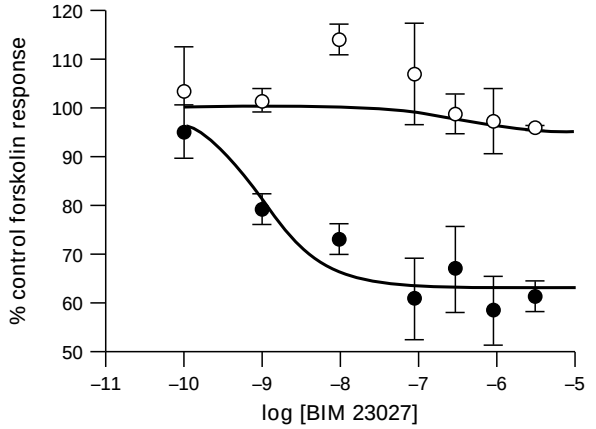

Figure 6 Effect of pretreatment with pertussis toxin on the inhibition of forskolin (10 μM)-stimulated increase in cyclic AMP by BIM-23027 in the presence of IBMX (0.5 mM). Neuro2A cells were pretreated with pertussis toxin (○, 500 ng ml^{-1}) for 16–18 h; control cells (●). Values are means ± s.e.mean of 3 separate determinations.

body (Schindler *et al*., 1996) has convincingly confirmed their presence.

The characteristics of the binding of [^{125}I]-BIM-23027 were evaluated, to enable appropriate design of functional assays. This is important, since it is known that some peptide ligands with very high affinities (dissociation constants in the picomolar range) do not dissociate readily (see Introduction). This would have particular implications for the design and interpretation of assays for receptor desensitization and ligand internalization, and also for the understanding of the interaction of somatostatin with its receptor in a whole-cell environment. We have not used whole-cell binding assays since the binding of agonist ligands is complicated by the internalization of the ligand (Koenig *et al*., 1996). Instead, the kinetics of [^{125}I]-BIM-23027 binding were studied in membranes from Neuro2A cells. The association kinetics closely follow a mono-exponential time course, at least within the first 4 h. However, in agreement with other reports, we have found that a significant proportion of specifically bound [^{125}I]-BIM-23027 does not dissociate

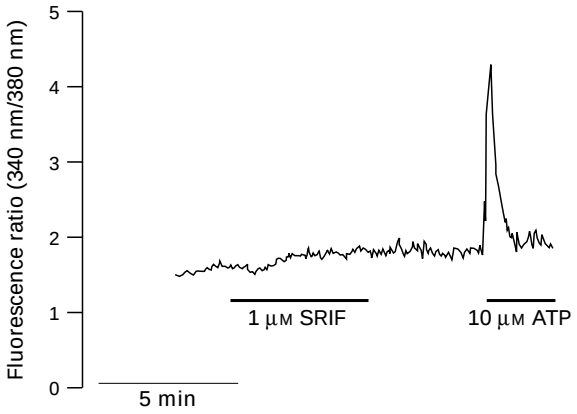

Figure 7 Effects of somatostatin and ATP on intracellular calcium ion concentration. Neuro2A cells were grown on glass coverslips and loaded with Fura-2-AM. They were then washed, mounted in a cuvette jacketed at 37°C and examined in a spectrofluorimeter. The coverslips were continuously perfused with HEPES-buffered Krebs pH 7.4 at 37°C. Somatostatin (1 μM) and ATP (10 μM) were each applied for a period of 5 min to the same coverslip. Note the response to ATP but not to somatostatin.

within 2 h at room temperature or below (Holloway *et al*., 1996; McKeen *et al*., 1996). This suggests that the receptor undergoes some conformational change subsequent to ligand binding which is not readily reversible at room temperature. As a result, competition binding would not be expected to be at equilibrium within 2 h and so the affinity estimates determined would not represent a true equilibrium dissociation constant. In contrast, increasing the temperature to 37°C allows almost complete dissociation within 2 h. At 37°C, the kinetic dissociation constant calculated from the association and dissociation rates (11 pM) agrees well with that derived from equilibrium saturation analysis (13 pM).

Addition of GTP and sodium chloride did not lead to total loss of high-affinity binding when assayed at room temperature. This is consistent with other studies which report a decrease in the amount of binding in the presence of GTP or GTP analogues (Reisine *et al*., 1993; Hershberger *et al*., 1994). However, in this study pertussis toxin treatment did virtually abolish high-affinity binding. Since we have shown that GTP and sodium chloride can lead to almost complete dissociation of bound radioligand in the presence of excess unlabelled ligand at 37°C but not at 15°C, it therefore seems likely that the reported inability of GTP and sodium chloride to completely remove high affinity binding (e.g. Reisine *et al*., 1993; Hershberger *et al*., 1994) may be an artefact of binding studies performed at room temperature. The dissociation of [^{125}I]-BIM-23027 in the presence of excess unlabelled SRIF and GTP and sodium chloride showed biphasic kinetics. This initial rapid phase may reflect a rapid conversion of the receptor to a low-affinity, undetectable state since addition of GTP and sodium chloride without excess unlabelled SRIF caused a rapid ($t_{1/2}$ less than 1 min) dissociation of ligand (data not shown).

Somatostatin receptors have been shown to couple to a variety of second messenger systems, although many of the reported studies have involved CHO-K1 cells expressing very high densities of receptor. In most natively-expressing cell lines and in brain tissue, the maximal inhibition of forskolin-stimulated adenylyl cyclase is generally less than 50% (50% in GH3 cells, Garcia & Myers, 1994; 35% inhibition in AtT20 cells, Mahy *et al*., 1988; 50% inhibition in GH_4C_1 cells, Presky & Schonbrunn, 1988; 10–20% inhibition in rat brain, Raynor & Reisine, 1992). In contrast, in transfected cells, maximal inhibition of 50–80% is often observed (Reisine *et al*., 1993, Hershberger *et al*., 1994; Williams *et al*., 1996). The reason for this discrepancy may be the low receptor density in natively-expressing cells. It is also known that there is a stringent re-

quirement for the presence of particular $G_{i\alpha}$ isoforms to mediate the coupling of somatostatin receptors to adenylyl cyclase (Patel *et al*., 1994; Liu *et al*., 1994). Therefore it is likely that if these particular isoforms are not present, or they are present in low abundance in a particular cell type, the efficiency of receptor-effector coupling will be low. Another explanation may be the presence of splice variants of the sst_2 receptor. Vanetti *et al*. (1993) and Reisine *et al*. (1993) have shown that the two splice variants of the sst_2 receptor, sst_{2a} (long form) and sst_{2b} (short form) have different efficiencies of coupling to adenylyl cyclase, with the sst_{2b} form showing greater efficiency. Vanetti *et al*. (1993) also claimed that the sst_{2a} receptor underwent marked desensitization whereas the sst_{2b} form did not. However, we were unable to demonstrate desensitization of the BIM-23027-mediated inhibition of adenylyl cyclase after pretreatment with 1 μM BIM-23027 for up to 2 h at 37°C (unpublished observations). It is not clear from the report of Vanetti *et al*. (1993) whether they measured the effects of receptor desensitization, receptor internalization or a combination of the two. Without further studies therefore we cannot surmise whether one or both splice variants are involved.

Somatostatin-induced increases in intracellular calcium via inositol phosphate production have been demonstrated in cells transfected with recombinant somatostatin receptors of the sst_2 and sst_5 subtypes (Akbar *et al*., 1994; Wilkinson *et al*., 1996). In contrast, in neuronally-derived, non-transfected cells, an effect of somatostatin on intracellular calcium relies upon prior administration of a submaximal concentration of an agonist which stimulates phospholipase C (Marin *et al*., 1991; Okajima & Kondo, 1992). In this study, we could not demonstrate a direct effect of SRIF-14 on intracellular calcium levels in Neuro2A cells, although the cells were responsive to ATP. Somatostatin receptors have also been shown to modulate levels of intracellular calcium by actions on voltage-gated calcium channels. For example, Liu *et al*. (1994) showed that somatostatin could inhibit Bay-K-8644-stimulated calcium current in GH_4C_1 cells. Also, in PC12 cells, Traina *et al*. (1996) showed that somatostatin affects the rise in intracellular calcium after depolarization induced by increased extracellular potassium through an inhibitory effect on voltage-dependent calcium channels. Although a dual 'self-cancelling' inhibitory and excitatory effect of somatostatin on intracellular calcium levels cannot be excluded in this study, this seems unlikely since we have confirmed in our own laboratories that sst_2 receptor activation will lead to increased intracellular calcium levels in CHO-K1 cells providing the receptor density is sufficiently high (G.F. Wilkinson, unpublished observations).

In conclusion, we have shown that Neuro2A neuroblastoma cells contain predominantly the sst_2 type of somatostatin receptor. Effectively complete reversibility of high-affinity binding and complete inhibition of binding by GTP and sodium chloride could be demonstrated when binding assays were performed at 37°C, but not at 15°C. Our data also indicate that somatostatin receptors in Neuro2A cells preferentially couple via pertussis toxin sensitive G proteins to adenylyl cyclase and that no effect on intracellular calcium mobilization was evident.

We would like to thank Diane Hall and Rejbinder Kaur for expert technical assistance. J.M.E. is grateful to the Wellcome Trust for financial support.

References

AKBAR, M., OKAJIMA, F., TOMURA, H., MAJID, M.A., YAMADA, Y., SEINO, S. & KONDO, Y. (1994). Phospholipase C activation and Ca^{2+} mobilization by cloned human somatostatin receptor subtypes 1-5, in transfected COS-7 cells. *FEBS Lett*., **348,** 192–196.

BRADFORD, M.M. (1976). A rapid and sensitive method for the quantitation of microgram quantities of protein utilizing the principle of protein-dye binding. *Anal. Biochem*., **72,** 248–254.

BUSCAIL, L., ESTEVE, J.-P., SAINT-LAURENT, N., BERTRAND, V., REISINE, T., O'CARROLL, A.-M., BELL, G.I., SCHALLY, A.V., VAYSSE, N. & SUSINI, C. (1995). Inhibition of cell proliferation by the somatostatin analogue RC-160 is mediated by somatostatin receptor subtypes SSTR2 and SSTR5 through different mechanisms. *Proc. Natl. Acad. Sci. U.S.A*., **92,** 1580–1584.

CASTRO, S.W., BUELL, G., FENIUK, W. & HUMPRHEY, P.P.A. (1996). Differences in the operational characteristics of the human recombinant somatostatin receptor types, sst_1 and sst_2, in mouse fibroblast (Ltk-) cells. *Br. J. Pharmacol*., **117,** 639–645.

GARCIA, P.D. & MYERS, R.M. (1994). Pituitary cell line GH3 express two somatostatin receptor subtypes that inhibit adenylyl cyclase: functional expression of rat somatostatin receptor subtypes 1 and 2 in human embryonic kidney cells. *Mol. Pharmacol*., **45,** 402–409.

HERSHBERGER, R.E., NEWMAN, B.A., FLORIO, T., BUNZOW, J., CIVELLI, O., LI, X.-J., FORTE, M., STORK, P.J.S. (1994). The somatostatin receptors SSTR1 and SSTR2 are coupled to inhibition of adenylyl cyclase in chinese hamster ovary cells via pertussis toxin-sensitive pathways. *Endocrinology*, **134,** 1277–1285.

HOFLAND, L.J., VAN KOETSVELD, P.M., WAAIJERS, M., ZUYDERWIJK, J., BREEMAN, W.A.P. & LAMBERTS, S.W.J. (1995). Internalization of the radioiodinated somatostatin analog [^{125}I-Tyr^3]-octreotide by mouse and human pituitary tumor cells: increase by unlabelled octreotide. *Endocrinology*, **136,** 3698–3706.

HOLLOWAY, S., FENIUK, W., KIDD, E.J. & HUMPHREY, P.P.A. (1996). A quantitative autoradiographical study on the distribution of somatostatin sst_2 receptors in the rat central nervous system using [^{125}I]-BIM-23027. *Neuropharmacology*, **35,** 1109–1120.

HOYER, D., BELL, G.I., BERELOWITZ, M., EPELBAUM, J., FENIUK, W., HUMPHREY, P.P.A., O'CARROLL, A.M., PATEL, Y.C., SCHONBRUNN, A., TAYLOR, J.E. & REISINE, T. (1995). Classification and nomenclature of somatostatin receptors. *Trends Pharmacol. Sci*., **16,** 81–116.

HOYER, D., LUBBERT, H. & BRUNS, C. (1994). Molecular pharmacology of somatostatin receptors. *Naunyn-Schmiedeberg's Arch. Pharmacol*., **350,** 441–453.

KLEUSS, C., HESCHELER, J., EWEL, C., ROSENTHAL, W., SCHULTZ, G. & WITTIG, B. (1991). Assignment of G-protein subtypes to specific receptors inducing inhibition of calcium currents. *Nature*, **353,** 43–48.

KOENIG, J.A., EDWARDSON, J.M. & HUMPHREY, P.P.A. (1996). Somatostatin receptors in neuro2A neuroblastoma cells: ligand internalization. *Br. J. Pharmacol*., **120,** 52–59.

LIU, Y.F., JAKOBS, K.H., RASENICK, M.M. & ALBERT, P.R. (1994). G protein specificity in receptor-effector coupling. *J. Biol. Chem*., **269,** 13880–13886.

MAHY, N., WOOLAKLIS, M., MANNING, D. & REISINE, T. (1988). Characteristics of somatostatin desensitization in the pituitary tumor cell line AtT-20. *J. Pharmacol. Exp. Ther*., **24,** 390–396.

MARIN, P., DELUMEAU, J.C., TENCE, M., CORDIER, J., GLOWINSKI, J. & PREMONT, J. (1991). Somatostatin potentiates the α1-adrenergic activation of phospholipase C in striatal astrocytes through a mechanism involving arachidonic acid and glutamate. *Proc. Natl. Acad. Sci. U.S.A*., **88,** 9016–9020.

MCKEEN, E., FENIUK, W., MICHEL, A.D., KIDD, A.J. & HUMPHREY, P.P.A. (1996). Identification and characterisation of heterogenous somatostatin binding sites in rat distal colonic mucosa. *Naunyn-Schmiedeberg's Arch. Pharmacol*., **354,** 543–549.

MERINEY, S.D., GRAY, D.B. & PILAR, G.R. (1994). Somatostatin-induced inhibition of neuronal Ca^{2+} current modulated by cGMP-dependent protein kinase. *Nature*, **369,** 337–339.

MUNSON, P.J. & RODBARD, D. (1980). LIGAND: a versatile computerised approach for characterization of ligand binding systems. *Anal. Biochem*., **107,** 220–239.

O'CARROLL, A.-M., RAYNOR, K., LOLAIT, S.J. & REISINE, T. (1994). Characterization of cloned human somatostatin receptor SSTR5. *Mol. Pharmacol*., **46,** 291–298.

OKAJIMA, F. & KONDO, Y. (1992). Synergism in cytosolic Ca^{2+} mobilization between bradykinin and agonists for pertussis toxin-sensitive G-protein-coupled receptors in NG108-15 cells. *FEBS Lett*, **301,** 223–226.

PATEL, Y.C., GREENWOOD, M.T., WARSZYNSKA, A., PANETTA, R. & SRIKANT, C.B. (1994). All five cloned human somatostatin receptors (hSSTR1-5) are functionally coupled to adenylyl cyclase. *Biochem. Biophys. Res. Commun.*, **198,** 605–612.

PATEL, Y.C. & SRIKANT, C.B. (1994). Subtype selectivity of peptide analogs for all five cloned human somatostatin receptors (hsstr1-5). *Endocrinology*, **135,** 2814–2817.

PRESKY, D.H. & SCHONBRUNN, A. (1988). Iodination of [Tyr^{11}]-somatostatin yields a super high affinity ligand for somatostatin receptors in GH4C1 pituitary cells. *Mol. Pharmacol.*, **34,** 651–658.

PRINZ, C., SACHS, G., WALSH, J.H., COY, D.H. & WU, S.V. (1994). The somatostatin receptor subtype on rat enterochromaffin-like cells. *Gastroenterology*, **107,** 1067–1074.

RAYNOR, K., MURPHY, W.A., COY, D.H., TAYLOR, J.E., MOREAU, J.P., YASUDA, K., BELL, G.I. & REISINE, T. (1993a). Cloned somatostatin receptors: identification of subtype-selective peptides and demonstration of high affinity binding of linear peptides. *Mol. Pharmacol.*, **44,** 838–844.

RAYNOR, K., O'CARROLL, A.M., KONG, H., YASUDA, K., MAHAN, L.C., BELL, G.I. & REISINE, T. (1993b). Characterization of cloned somatostatin receptors SSTR4 and SSTR5. *Mol. Pharmacol.*, **44,** 385–392.

RAYNOR, K. & REISINE, T. (1992). Differential coupling of somatostatin-1 receptors to adenylyl cyclase in the rat striaturm vs. the pituitary and other regions of the rat brain. *J. Pharmacol. Exp. Ther.*, **260,** 841–848.

REISINE, T., KONG, H., RAYNOR, K., YANO, H., TAKEDA, J., YASUDA, K. & BELL, G.I. (1993). Splice variant of the somatostatin receptor 2 subtype, somatostatin receptor 2B couples to adenylyl cyclase. *Mol. Pharmacol.*, **44,** 1008–1015.

SCHINDLER, M., SELLERS, L.A., HUMPHREY, P.P.A. & EMSON, P.C. (1996). Immunohistochemical localisation of the somatostatin $sst_{2(a)}$ receptor in the rat brain and spinal cord. *Neuroscience*, (in press).

SCHWEITZER, P., MADAMBA, S. & SIGGINS, G.R. (1990). Arachidonic acid metabolites as mediators of somatostatin-induced increase of neuronal M-current. *Nature*, **346,** 464–467.

TAYLOR, J.E., THEVENIAU, M.A., BASHIRZADEH, R., REISINE, T. & EDEN, P.A. (1994). Detection of somatostatin receptor subtype 2 (SSTR2) in established tumors and tumor cell lines: evidence for SSTR2 heterogeneity. *Peptides*, **15,** 1229–1236.

TRAINA, G., CANNISTRATO, S. & BAGNOLI, P. (1996). Effects of somatostatin on intracellular calcium concentration in PC12 cells. *J. Neurochem.*, **66,** 485–492.

VANETTI, M., VOGT, G. & HOLLT, V. (1993). The two isoforms of the mouse somatostatin receptor (mSSTR2A and mSSTR2B) differ in coupling efficiency to adenylate cyclase and in agonist-induced receptor desensitisation. *FEBS Lett.*, **331** 260–266.

WHITE, R.E., SCHONBRUNN, A. & ARMSTRONG, D.L. (1991). Somatostatin stimulates Ca^{2+}-activated K^+ channels through protein dephosphorylation. *Nature*, **351,** 570–572.

WILKINSON, G.F., THURLOW, R.J., SELLERS, L.A., COOTE, J.E., FENIUK, W. & HUMPHREY, P.P.A. (1996). Potent antagonism by BIM-23056 at the human recombinant somatostatin sst5 receptor. *Br. J. Pharmacol.*, **118,** 445–447.

WILLIAMS, A.J., MICHEL, A.D., COOTE, J.E., SELLERS, L., FENIUK, W. & HUMPHREY, P.P.A. (1996). Characterisation of the human recombinant sst5 receptor in CHO-K1 cells by quantification of guanosine-5′-O-(3-[35]-thio)triphosphate binding. *Br. J. Pharmacol.*, **117,** 10P.

WU-WONG, J.R., CHIOU, W.J., MAGNUSON, S.R. & OPGENORTH, T.J. (1995). Endothelin receptor in human astrocytoma U373MG cells: binding, dissociation, receptor internalization. *J. Pharmacol. Exp. Ther.*, **274,** 499–507.

(Received July 3, 1996
Revised September 11, 1996
Accepted September 19, 1996)